JOURNAL OF AGRICULTURAL AND FOOD CHEMISTRY
ARTICLE

J. Agric. Food Chem. 2010, 58, 11097–11104 11097
DOI:10.1021/jf1024533

Formation of Semi-compound C-Type Starch Granule in High-Amylose Rice Developed by Antisense RNA Inhibition of Starch-Branching Enzyme

Cunxu Wei,[†,‡] Fengling Qin,[†] Weidong Zhou,[§] Yifang Chen,[§] Bin Xu,[§] Youping Wang,[†] Minghong Gu,*[,‡] and Qiaoquan Liu*[,‡]

[†]College of Bioscience and Biotechnology, [‡]Key Laboratories of Crop Genetics and Physiology of the Jiangsu Province and Plant Functional Genomics of the Ministry of Education, and [§]Testing Center, Yangzhou University, Yangzhou 225009, China

Cereal starch granules with high-amylose and resistant starch (RS) always show irregular morphology and special crystalline structure, but their formation during grain development is not yet clear. In our previous studies, we had generated a transgenic rice line (TRS) enriched with amylose and RS, which contained semi-compound starch showing a C-type crystalline structure. In this study, the formation of semi-compound C-type starch granule during TRS endosperm development was carefully investigated with light, scanning electron, and transmission electron microscopes and X-ray powder diffraction. The results showed that the TRS starch subgranules, each with a central hilum, were individually initiated in amyloplast and showed an A-type crystal at the early stage of starch granule development, which was similar to that in its wild type. However, with the endosperm development, the amylose content in TRS endosperm starch increased and the B-type starch crystal was deposited in the periphery of subgranules; then, the adjacent subgranules fused together and finally formed a continuous outer layer band surrounding the entire circumference of the starch granule. Accordingly, a mechanistic model for the formation of semi-compound C-type starch granules is proposed.

KEYWORDS: Rice (*Oryza sativa* L.); high-amylose starch; C-type starch; endosperm development; starch granule formation

INTRODUCTION

Cereal storage starch is a major source of nourishment for humans. Resistant starch (RS) is a portion of starch that cannot be hydrolyzed and functions as a prebiotic for bacterial fermentation in the large intestine (*1*). Therefore, RS has been reported to provide many health benefits for humans; e.g., RS-enriched food can lower the glycemic and insulin responses and reduce the risk for developing type-2 diabetes, obesity, and cardiovascular disease (*2*).

In comparison to normal diets, there is much more RS in the diet containing starches, which retains granular structures that are naturally resistant to digestion, especially for the granules with high amylose content (*3*). Therefore, many high-amylose crop varieties had been developed via mutation or transgenic breeding approaches (*4*−*9*). Some of them have been proven to contain a high level of RS and show potential health benefits. For examples, high-amylose barley and wheat grains have significant potential to improve health by the reduction of plasma cholesterol and the production of increased large-bowel short-chain fatty acids (*7*, *8*).

*To whom correspondence should be addressed. Telephone: +86-514-87996648. E-mail: gumh@yzu.edu.cn (M.G.); qqliu@yzu.edu.cn (Q.L.).

However, the starch granules with very high amylose often show an irregular shape when compared to normal ones. For instance, the normal maize starch granules are spherical and angular, whereas high-amylose *ae* and GEMS-0067 mutants consist of about 7% and up to 32% elongated granules, respectively (*10*). In potato tubes, suppression of starch-branching enzymes (SBEs) resulted in a very high-amylose phenotype, but it had a severe effect on the starch granule morphology with multi-lobed or fissured shapes (*5*). In normal rice endosperm, starch granules are developed in the amyloplasts, and when mature, 20−60 individual starch subgranules are tightly packed and formed as compound starch granules. However, in the high-amylose rice line Goami 2 (previously known as Suweon 464), the adjacent starch subgranules, which are located at the periphery of compound starch, were fused and formed a thick band or wall encircling the entire circumference (*11*).

Regularly, the normal cereal starches always show an A-type crystalline structure (*12*), and cereal starches with high amylose usually present a B-type crystalline structure (*4*, *6*, *13*). However, not all of the high-amylose cereal starches are B-type. For example, some rice and barley mutants with high amylose were identified to contain a typical A-type X-ray powder diffraction (XRD) pattern (*9*, *14*). Besides, C-type crystalline was also observed in several high-amylose cereal starches, although in rare

Published on Web 09/24/2010

cases. Cheetham and Tao (*13*) reported that the crystal type of maize starch could be varied from A to B via C type when amylose increased and the transition occurred at about 40%.

For the high-amylose crop starches, there are many studies on their morphological structure and crystalline property as mentioned above, but the formation of these starch granules is not yet clear. Kim et al. (*15*) compared the ultrastructure of starch granules between high-amylose rice mutant Goami 2 and its wild type, but the research was only focused on 20 days after flowering (DAF) when starch endosperm is close to maturity. The development of high-amylose starch granules is not reported. Recently, Jiang et al. (*16*) used light, confocal laser-scanning, scanning electron, and transmission electron microscopes to observe the formation of elongated starch granules in high-amylose maize. Their results showed that many starch granules, each with hilum and growth rings, were initiated in amyloplast and then fused by forming antiparallel amylose double helices between two growing granules. These fused starch granules resulted in the continuous outer layer, which prevents amyloplast division and forms the elongated starch granules (*16*). However, their study was only focused on the subaleurone layers of kernel at 20 DAF.

Recently, we have developed several high-amylose transgenic rice lines (TRSs) by antisense RNA inhibition of SBEs (*17*, *18*). These transgenic rice grains are rich in RS and have been proven to show a significant potential to improve the large-bowel health in rats (*19*). Our results from micro- and ultrastructure studies revealed that the high-amylose TRS starch is semi-compound starch granule and consists of many subgranules surrounded by a continuous outer layer band (*18*). Interestingly, these high-amylose rice starches show a C-type crystalline, a combination of A- and B-type allomorphs (*20*). The A- and B-type allomorphs coexisted in the individual C-type starch granule. The A-type allomorph basically existed in the interor part of the subgranules, which was surrounded by the B-type allomorph in the peripheral part of subgranules and the surrounding band of starch granule (Wei et al., manuscript submitted). Thus, it is of great interest to understand how these semi-compound C-type starch granules are formed during kernel development.

In this study, we used different microscopic approaches to reveal the internal structures and formation of C-type starch granules during endosperm development. Besides, the crystalline property of our high-amylose starches during grain development was also carefully investigated using the XRD technique. On the basis of these data, we propose a mechanistic model for the formation of semi-compound C-type starch granule in high-amylose rice. This research could add to our understanding of not only semi-compound starch, C-type starch, and crystal allomorph positions of high-amylose cereal starch but also the reason for high-amylose starch resistance to hydrolysis.

MATERIALS AND METHODS

Plant Materials. A TRS with high amylose and RS and its wild-type Te-qing (TQ) were used in this study. TRS was generated from the indica rice cultivar TQ after transgenic inhibition of two SBEs (SBEI and SBEIIb) through the antisense RNA technique and held the homozygous transgene (*17*). The transgenic line in T8 generation and its wild type were cultivated in the experiment field of Yangzhou University, Yangzhou, China, in 2009. Individual flowers were tagged at flowering. The caryopses were harvested at various DAF during seed development.

Specimen Preparation for Light Microscope (LM) and Transmission Electron Microscope (TEM). The collected caryopses at different development stages were used to prepare two types of specimens: one for the conventional glutaraldehyde−osmium tetroxide (GA−OsO_4) fixation and another for the potassium permanganate ($KMnO_4$) fixation. The latter is a better method for membrane structure investigation (*21*). For GA−OsO_4 fixation, each of the harvested grains was transversely cut with a razor blade in the mid-region of the kernel to obtain small tissue blocks. Tissue blocks were then immediately fixed in a fixation solution (2.5% glutaraldehyde and 4% paraformaldehyde in 0.1 M phosphate buffer at pH 7.2) for 2 h at room temperature and then held overnight at 4 °C. After three changes of washing (15 min each) with the phosphate buffer, the blocks were postfixed in 1% OsO_4 for 2.5 h at room temperature. The blocks were washed, dehydrated, and embedded in Epon 812 resin. For $KMnO_4$ fixation, tissue blocks were immediately immersed in a 1.2% $KMnO_4$ solution containing 0.5% NaCl in barbital sodium buffer for 4 h at 4 °C. After $KMnO_4$ fixation, samples were washed 3 times (20 min each) with a 0.5% NaCl solution at 4 °C and then passed once through 35% ethanol. Next, the samples were further fixed in 70% ethanol for 12 h at 4 °C. After ethanol fixation, the samples were dehydrated and embedded in Epon 812 resin.

The semi-thin sections from GA−OsO_4 fixation samples in 1 μm thickness were cut with a glass knife on a Leica Ultrathin Microtome (EM UC6), stained with periodic acid−Schiff (PAS) reagent, and observed on an Olympus BH2 LM. Slightly thicker ultra-thin sections in 100 nm thickness were cut with a diamond knife on a Leica Ultrathin Microtome (EM UC6) and post-stained with uranyl acetate and lead citrate. The sections were visualized and photographed with Philips Tecnai 12 TEM at 100 kV.

Specimen Preparation for Scanning Electron Microscope (SEM). Harvested caryopses were immediately fixed in the fixation solution (2.5% glutaraldehyde and 4% paraformaldehyde in 0.1 M phosphate buffer at pH 7.2) for 2 h at room temperature and then held at 4 °C. After fixation, the samples were washed 3 times with phosphate buffer, successively dehydrated in gradient ethanol, and substituted with isoamyl acetate. Then, the samples were dried in a CO_2 critical point dryer. The dried grains were fractured in the mid-region of the kernel with a razor blade by applying a slight pressure on the top of the grain. During fracturing, the efforts were made to produce no physical contact between the razor blade and the fractured surface of the internal endosperm tissues. Fractured grains, with the fractured surface upward, were mounted on the specimen stub and sputter-coated with gold before viewing with a Philips XL30 ESEM at 20 kV.

Isolation of Starch Granules and Analysis of Amylose Content. Developing starch granules were isolated as previously described (*20*). The apparent amylose content was determined using a colorimetric method with iodine−potassium iodide (*22*).

XRD Analysis. XRD analysis of developing starch granules was carried out on an XRD (D8, Bruker, Germany) as previously described (*20*). Moisture of the hydrated starch samples was about 20%. The degree of crystallinity of samples was quantitatively estimated following the method of Nara and Komiya (*23*), with minor modification. A smooth curve, which connected peak baselines, was computer-plotted on the diffractograms (**Figure 5**). The area of peaks at 5.6°, 15°, 17°, 18°, 20°, and 23° 2θ above the smooth curve was taken as the crystalline portion, and the lower area between the smooth curve and a linear baseline, which connected the two points of intensity at 2θ of 30° and 4° in the samples was taken as the amorphous section. The upper diffraction peak area and total diffraction area over the diffraction angle 4−30° 2θ were integrated using JEDA-801D morphological image analysis software (Jiangsu JEDA Science-Technology Development Co., Ltd., Nanjing, China). The ratio of the upper area to the total diffraction area was taken as the degree of crystallinity.

RESULTS AND DISCUSSION

LM Study of Developing Starch Granules. Starch in normal rice endosperm is compound starch granule (*11*, *24*). At the early stage of TQ endosperm development, many starch subgranules, each with a hilum at the center of the subgranule, were individually initiated in an amyloplast (**Figure 1A**). With seed development, endosperm cells were full of amyloplasts, and many individual polygonal starch subgranules were tightly packed in each amyloplast (**Figure 1B**). Therefore, TQ starch was a typical compound starch. However, in high-amylose TRS mature seed, there are mainly the large voluminous, elongated, and internal hollow starch granules that we previously reported (*18*). For the development of a large voluminous starch granule, the TRS starch subgranules,

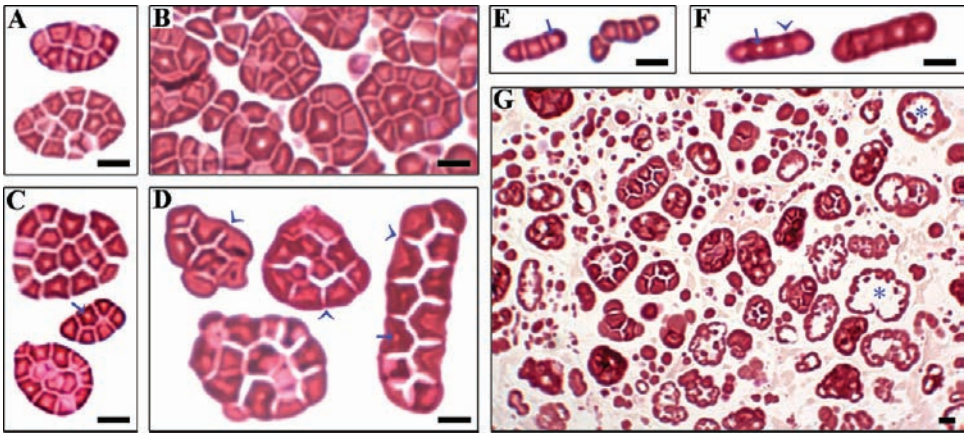

Figure 1. LM micrographs of developing starch granules stained by PAS reagent: (A and B) TQ and (C−G) TRS. (A and C) Starch at 4 DAF, showing that many starch subgranules, each with a central hilum, individually existed in one amyloplast. (B) Starch in endosperm cells at 12 DAF, showing that endosperm cells were full of compound starch and the adjacent subgranules were not fused, forming a continuous outer layer band surrounding the entire circumference of the starch granule in amyloplast. (D) Large voluminous starch at 12 DAF, showing that adjacent subgranules were fused, forming a continuous outer layer band surrounding the entire circumference of the starch granule in amyloplast. (E) Elongated starch at 4 DAF, showing that some linearly arranged starch subgranules, each with a central hilum, individually existed in one amyloplast. (F) Elongated starch at 12 DAF, showing that subgranules were fused, forming one elongated starch granule. (G) Subaleurone layer cells at 24 DAF, showing that there were many large voluminous starch granules, small elongated starch granules, and internal hollow starch granules in endosperm cells. The arrow shows the hilum. The arrow head shows the band. The star shows the internal hollow starch granules. Scale bar = 5 μm.

each with a hilum at the center of the subgranule, were also individually initiated in an amyloplast at the early stage of starch development (**Figure 1C**) and similar to that of wild-type TQ (**Figure 1A**). With the development, subgranules located at the periphery of a starch granule fused and formed a continuous outer layer band surrounding the entire circumference of the granule (**Figure 1D**). For the case of elongated starch granule development, many linearly arranged small starch subgranules were first individually initiated in an amyloplast (**Figure 1E**) and then fused into one elongated starch granule (**Figure 1F**). Besides, some internal hollow starch granules were observed after 12 DAF and mainly distributed in subaleurone layer cells (**Figure 1G**).

SEM Study of the Developing Starch Granule. The cereal endosperm consists of the aleurone layer, the subaleurone layer, and the starchy endosperm layer (*25*). **Figure 2** shows the submicroscopic structure of starch granules during seed development. At the early stage of TQ endosperm development, many polygonal starch subgranules individually existed in an amyloplast (**Figure 2A**). For mature TQ seed, endosperm cells were full of compound starch granules. The intracellular fractured surface of TQ mature endosperm produced an uneven and rough surface morphology because of the exposure of unevenly cleaved starch granules of various size and shapes. Compound starch granules were either unsplit or partially split. Partially split compound starch granules exposed the presence of individual starch subgranules with sharp angles and edges (**Figure 2B**). For TRS starch, at the early stage of starch development, many polygonal starch subgranules also individually existed in one amyloplast in the endosperm cell (**Figure 2C**), similar to that of wild-type TQ (**Figure 2A**). At 12 DAF, many irregular and elongated starch granules were observed in subaleurone layer cells (**Figure 2D**). For mature seed, the starchy endosperm cell was full of large voluminous starch granules without sharp angles and edges (**Figure 2E**), while the subaleurone layer cell was filled with mainly irregular and elongated starch granules (**Figure 2F**).

TEM Study of the Developing Starch Granule. To understand starch granule formation during kernel development, developing endosperm tissues were harvested and used for TEM studies. The ultrastructure of developing normal rice starch granules fixed by GA−OsO_4 has been reported in many papers (*11*, *15*, *24*). The results of developing a TQ starch granule fixed by GA−OsO_4 (data not shown) were similar to the literature. The ultrastructure of developing TRS starch granules fixed by GA−OsO_4 is shown in **Figure 3**. One amyloplast contained many starch subgranules. Most of them were polygonal at 4 DAF. These subgranules individually existed in an amyloplast (**Figure 3A**), similar to that of normal rice (*24*). At 6 DAF, the sizes of subgranules increased and the structure and component of the peripheral part of the subgranule were obviously different from that of the internal part (panels **B**−**E** of **Figure 3**). The external portions of most subgranule peripheral parts were serrated in a radial direction with deep and narrow clefts of various depths and widths, exhibiting a saw- or comb-like profile, as reported by Kim et al. (*11*). The structure from adjacent subgranules was interrelated, interacted on each other (panels **D** and **E** of **Figure 3**), and then fused, forming the continuous outer layer band, which surrounded the entire circumference of starch subgranules (**Figure 3F**). Finally, the amyloplast membrane was degraded (**Figure 3G**). **Figure 3G** showed that seven starch subgranules, each with a central hilum and many concentric growth rings, were fused into one starch granule. The outer growth rings were also observed in the peripheral band of the starch granule (**Figure 3G**), which suggested that the starch granule was semi-compound starch according to the concept of semi-compound starch (*24*, *26*). During endosperm development, we also observed the formation of some irregular starch granule (**Figure 3H**), elongated starch granule (**Figure 3I**), and internal hollow starch granule (**Figure 3J**) in amyloplast.

Although the internal ultrastructure of the starch granule was observed with GA−OsO_4 fixation, it was difficult to observe the amyloplast membrane. $KMnO_4$ is a better fixative for membrane lipids, although it is poor for protein and polysaccharide. In addition, its osmotic ability is very high to the cell membrane. Thus, it can rapidly fix the membrane structure within a 1−2 min duration and increase the contrast of the membrane structure. In comparison to conventional GA−OsO_4 fixation, $KMnO_4$ is a better method for the membrane structure (*21*). The ultrastructure of developing TQ and TRS starch granules fixed by $KMnO_4$

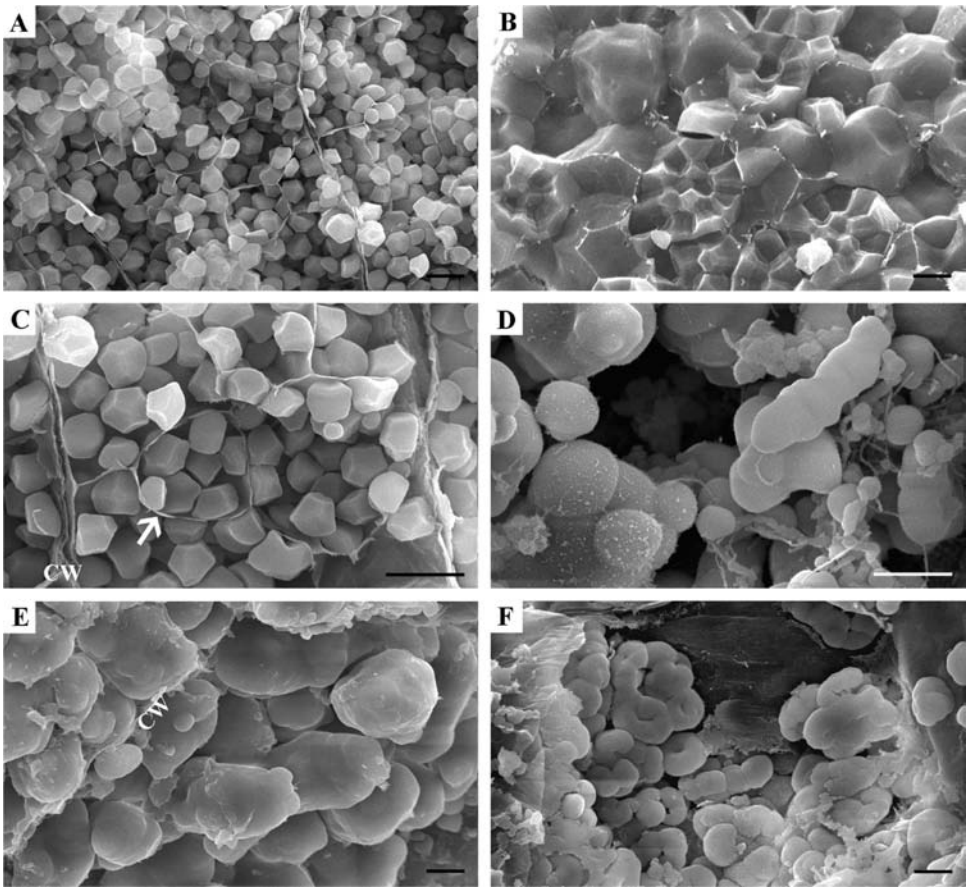

Figure 2. SEM micrographs of developing endosperm: (A and B) TQ and (C−F) TRS. (A and C) Endosperm cell at 4 DAF, showing that many starch subgranules individually existed in one amyloplast. (B) Starchy endosperm cell of the mature seed, showing unsplit and partially split compound starch granules, exposing the presence of individual starch subgranules with sharp angles and edges. (D) Subaleurone layer cell at 12 DAF, showing irregular and elongated starch granules. (E) Starchy endosperm cell of the mature seed, showing large voluminous starch granules. (F) Subaleurone layer cell of the mature seed, showing irregular starch granules. The arrow shows the amyloplast membrane. CW = cell wall. Scale bar = 5 μm.

is shown in **Figure 4**. For TQ developing endosperm, we could clearly observe that many ellipsoidal starch subgranules developed in one amyloplast at 2 DAF (**Figure 4A**). At 6 DAF, the sizes of starch subgranules increased. They became polygonal and individually existed in one amyloplast (**Figure 4B**). At 12 DAF, the endosperm cell was nearly full of compound starches, in which polyhedral starch subgranules were tightly packed but separated and adjacent subgranules were not fusing to each other to form the continuous band encircling the entire circumference of the compound starch (**Figure 4C**). For TRS developing endosperm, we could also clearly observe that many amyloplasts, each with many individual starch subgranules, were distributed around the cell nucleus and cell wall at 2 DAF (**Figure 4D**). At 4 DAF, the sizes of starch subgranules increased. Some protrusions, in which some small starch subgranules were linearly arranged, were observed from the amyloplast membrane (panels **E**−**G** of **Figure 4**). These protrusions were speculated to be a kind of proliferation way of amyloplast to form the elongated starch. **Figure 4F** showed the development of elongated starch granule. Some endosperm cells contained fewer amoeba-like amyloplasts. Some regions of these amyloplast membranes protruded or invaginated, which was also speculated to form new amyloplast (panels **H** and **I** of **Figure 4**). Some fusing starch subgranules were also observed in amyloplast (**Figure 4J**). Panels **K** and **L** of **Figure 4** showed the fused granules with a continuous outer layer band surrounding the entire circumference of the starch granule. The amyloplast membrane was clearly observed.

Crystalline Properties of the Developing TRS Starch Granule. The XRD spectra of developing starch granules are given in **Figure 5A**. The starch at 4 DAF displayed strong reflections at 15°, 17°, 18°, and 23° 2θ, which were typical peaks of the A-type crystal, as classified by Cheetham and Tao (*13*). The starch at 6 and 9 DAF appeared to be a C_A type (type C near the A type). Because the C type has been suggested as a mixture of A and B types, the C pattern is classified as closer to the A type (C_A) or closer to the B type (C_B). The patterns of starches at 6 and 9 DAF were the same as the A-type crystal, except for the presence of the medium peak of 5.6° 2θ, which indicated the occurrence of B-type crystalline regions in starch, and the lower peak of 18° 2θ. The starches at 12 and 18 DAF exhibited a typical C-type crystal, with the high and sharp peak of 17° 2θ and medium peaks of 5.6°, 15°, 20°, and 23° 2θ, without the peak of 18° 2θ, which was characteristics of both A- and B-type crystals (*13*). Therefore, the diffraction pattern of starch was C-type. The peak at 20° 2θ indicated the crystalline amylose−lipid complexes (*13*). With the increase of development, obvious increases of 5.6° and 20° 2θ could be observed. The increase of the 5.6° 2θ peak represented the transformation of the A type or amorphous region into B-type crystalline regions. The increase of the 20° 2θ peak indicated that more crystalline amylose−lipid complexes were generated. Therefore, we could postulate that the development of starch granules was accompanied by the formation of more B-type crystalline regions and crystalline amylose−lipid complexes. In turn, these behaviors resulted in the C-type crystal. The degree of crystallinity of developing starch was given in **Figure 5B**. The starch at 4 DAF

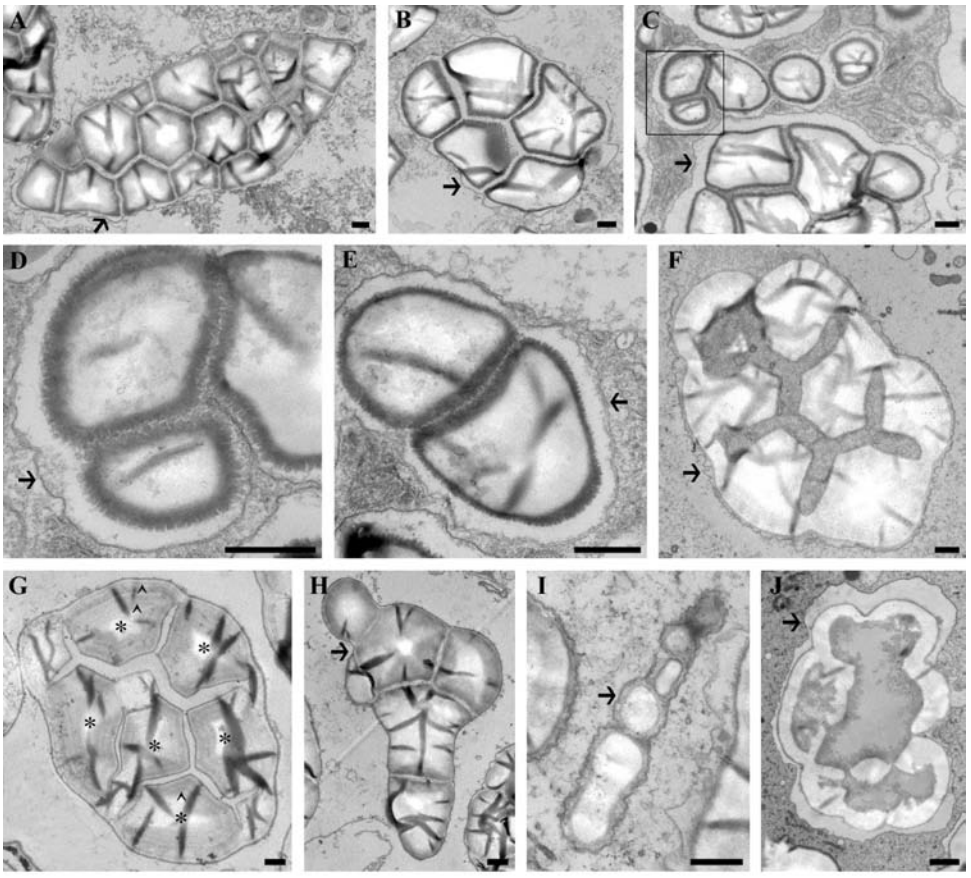

Figure 3. TEM micrographs of developing TRS endosperm fixed by GA−OsO_4. (A) Starch at 4 DAF, showing that many starch subgranules individually existed in one amyloplast. (B−E) Starch at 6 DAF, showing that there were obvious differences between the peripheral part and internal part of subgranules (B and C). Adjacent subgranules were fusing each other (D and E). (D) Higher magnification view of the squared area shown in panel C. (E) Clearly double membrane of amyloplast. (F) Starch granule at 12 DAF, showing that the continuous band surrounded starch subgranules in amyloplast. (G) Starch granule without the amyloplast membrane at 18 DAF, showing that many starch subgranules, each with a central hilum and growth rings, were surrounded by a continuous band with integrated outer layer growth rings. (H) Irregular starch in amyloplast at 4 DAF. (I) Elongated starch at 4 DAF, showing that some starch subgranules were linearly arranged in amyloplast. (J) Internal hollow starch in amyloplast at 12 DAF. The arrow shows the amyloplast membrane. The arrow head shows the growth rings. The star shows the hilum. Scale bar = 1 μm.

showed the highest degree of crystallinity, and then the degrees of crystallinity decreased with starch development.

Amylose Contents of the Developing TRS Starch Granules. The amylose contents of the developing endosperm starches are shown in **Figure 5B**. The amylose content of the endosperm starch increased from 21.35% at 4 DAF to 57.21% at 18 DAF. The mature endosperm starch had similar amylose content (58.32%) to the starch isolated at 18 DAF. It is known that the starch granule is synthesized by apposition, from the hilum toward the periphery (*27*). Thus, the core of the starch granule corresponds to the small granule synthesized at the early stage of the starch granule development. Granule-bound starch synthase I (GBSS I) is the primary enzyme for amylose biosynthesis in the storage organ. The mRNA of rice GBSS I increased with the development of endosperm (*28*), and TRS starch-branching enzymes (SBEI and SBEIIb) were inhibited at middle and later stages of the kernel development (*17*). Therefore, the amylose contents gradually increased with endosperm cell development. This result also indicated that the outer layer of starch granules contained a higher amylose content than the inner part of the granules, which was in accordance with the 8-amino-1,3,6-pyrenetrisulfonic acid (APTS)-stained starch granules reported by Wei et al. (*18*).

Proposed Formation Mechanism of the Semi-compound C-Type Starch Granule. According to the changes of morphological structure, crystal pattern, and amylose content of the developing starch granule, a proposed model of semi-compound C-type starch granule formation is shown in **Figure 6**. First, many starch subgranules, each with a central hilum, were initiated in one amyloplast with double membrane. The amylose content was low, and the crystalline was A-type (**Figure 6a**). Second, the size of the subgranule increased, and the peripheral parts of the subgranule were high-amylose B-type crystal starch components. The starch showed C_A-type crystal (**Figure 6b**). Then, adjacent granules began fusing (**Figure 6c**), and these fused subgranules produced a continuous outer layer band with growth rings (**Figure 6d**), which consisted of more amylose (*18*). The band had resistance to acid hydrolysis (*20*), which retained the B-type semi-crystalline structure and, in turn, maintained the granular shape of the semi-compound starch granules after 2.2 M HCl hydrolysis for 20 days (Wei et al., manuscript submitted). Finally, the amyloplast membrane was degraded, and the starch showed semi-compound C-type crystal starch (**Figure 6e**). In normal rice starch granules, many starch subgranules, each with a central hilum, were initiated in one amyloplast with double membrane. The sizes of subgranules increased with development; however, they did not fuse and kept individual distribution in amyloplast. Then, the amyloplast membrane was degraded (*24*). Therefore, normal rice starch was compound A-type crystal starch (*20*, *24*).

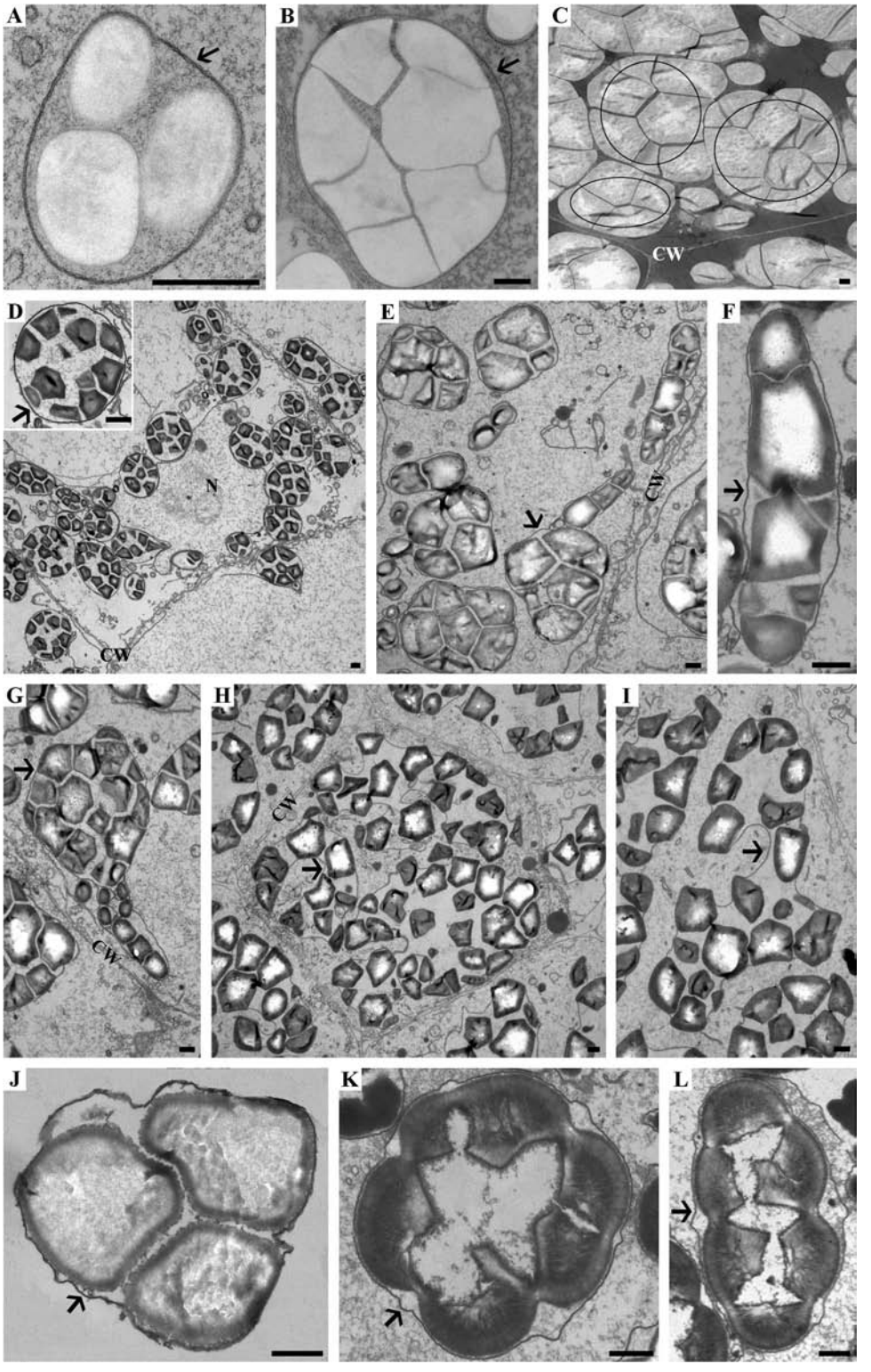

Figure 4. TEM micrographs of developing endosperm fixed by potassium permanganate: (A−C) TQ and (D−L) TRS. (A) Starch at 2 DAF, showing many ellipsoidal starch subgranules in one amyloplast. (B) Starch at 6 DAF, showing many polyhedral starch subgranules in one amyloplast. (C) Starch at 12 DAF, showing that adjacent starch subgranules in amyloplasts were separated and not fused, forming a continuous outer layer band. (D) Overview of the endosperm cell at 2 DAF. The inset was the magnified image of one amyloplast. (E−I) Starch at 4 DAF, showing that some amyloplast membranes protruded to form the elongated starch (E−G) and some endosperm cells contained fewer amoeba-like amyloplasts (H and I). (J) Starch at 6 DAF, showing that some subgranules were fusing. (K and L) Starch at 12 DAF, showing that adjacent granules were fused, forming a continuous outer layer band surrounding the entire circumference of the starch granule. The arrow shows the amyloplast membrane. CW = cell wall. N = nucleus. The ring shows the compound starch. Scale bar = 1 μm.

Recently, Jiang et al. (*16*) proposed a mechanism of the development of elongated starch granules in high-amylose maize. They thought that the amylose molecules of an individual granule in the amyloplast interacted and formed antiparallel double helices with amylose molecules of an adjacent granule. These double helices bound the two adjacent granules together, and then they were fused, forming one elongated starch granule that had a continuous high-amylose outer layer. In normal maize

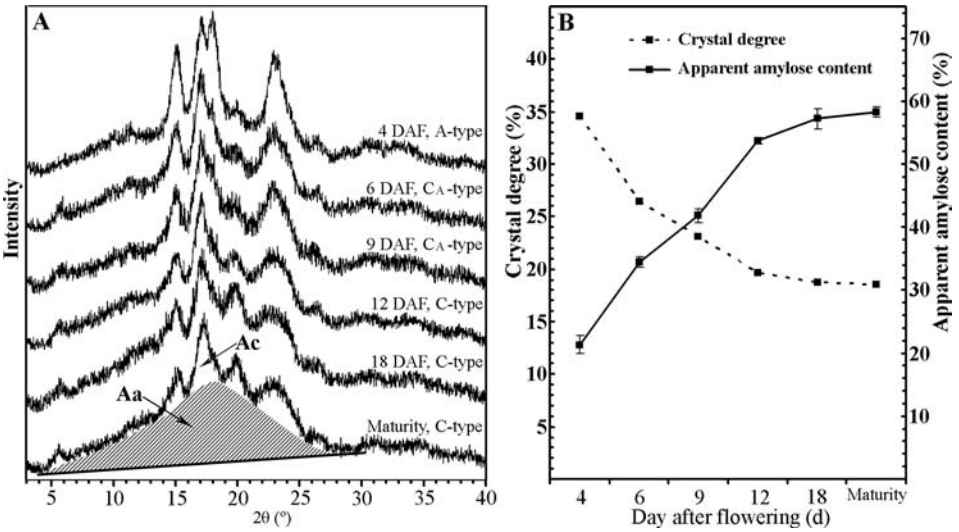

Figure 5. XRD spectra and amylose contents of TRS starch granules isolated from developing endosperm. (A) XRD spectra, showing a transition of the crystalline type from A to C_A to C type during endosperm development. The Aa and Ac refer to the amorphous and crystallized areas, respectively, on the XRD spectra. Endosperm development time and starch crystal type are indicated next to each XRD spectrum. (B) Relative crystal degrees and amylose contents of developing starch granules.

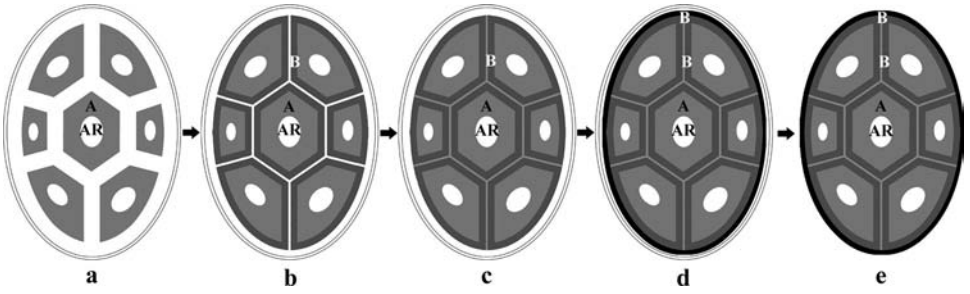

Figure 6. Proposed model of semi-compound C-type starch granule formation. (a) Many starch subgranules (A-type crystal), each with a central hilum, are initiated in one amyloplast. (b) B-Type crystal is deposited in the periphery of the subgranule. (c) Adjacent subgranules start fusion. (d) Adjacent subgranules produce a continuous outer layer band, which is B-type crystal. (e) The double amyloplast membrane is degraded. A, A-type starch crystal; AR, amorphous region of the starch granule, which is around the hilum; B, B-type starch crystal.

starch granules, amylose molecules were separated by amylopectin molecules because of the low concentration of amylose. The branch chains of amylopectin molecules were not long enough to form stable antiparallel double helices between two adjacent granules in the normal maize amyloplast (*29*). Our results were in accordance with the fusion mechanism of high-amylose starch granule (*16*). To the best of our knowledge, this mechanistic model assisted with the understanding of the formation of semi-compound C-type crystal starch granules and RS formation in high-amylose rice starch (*18*, *20*), which was also in accordance with the allomorph position of these starches (Wei et al., manuscript submitted).

In conclusion, the formation of semi-compound C-type crystal starch granules in high-amylose rice was carefully investigated by LM, SEM, and TEM during TRS rice endosperm development. Starch subgranules, each with a central hilum, were individually initiated in amyloplast at the early stage of granule development, and then adjacent subgranules fused together, forming a continuous outer layer band surrounding the entire circumference of the starch granule. During this development, the starch crystalline changed from A to C via C_A type and the amylose content significantly increased. According to these results, a mechanistic model for semi-compound C-type starch granule formation was proposed, which could add to our understanding of not only semi-compound starch, C-type starch, and the crystal allomorph position of high-amylose cereal starch but also the reason for starch resistance to hydrolysis.

ABBREVIATIONS USED

DAF, day after flowering; GA−OsO_4, glutaraldehyde−osmium tetroxide; LM, light microscope; PAS, periodic acid−Schiff; RS, resistant starch; SBE, starch-branching enzyme; SEM, scanning electron microscope; TEM, transmission electron microscope; XRD, X-ray powder diffraction.

LITERATURE CITED

(1) Englyst, H. N.; Macfarlane, G. T. Breakdown of resistant and readily digestible starch by human gut bacteria. *J. Sci. Food Agric.* **1986**, *37*, 699−706.
(2) Nugent, A. P. Health properties of resistant starch. *Nutr. Bull.* **2005**, *30*, 27−54.
(3) Rahman, S.; Bird, A.; Regina, A.; Li, Z. Y.; Ral, J. P.; McMaugh, S.; Topping, D.; Morell, M. Resistant starch in cereals: Exploiting genetic engineering and genetic variation. *J. Cereal Sci.* **2007**, *46*, 251−260.
(4) Yano, M.; Okuno, K.; Kawakami, J.; Satoh, H.; Omura, T. High amylose mutants of rice, *Oryza sativa* L. *Theor. Appl. Genet.* **1985**, *69*, 253−257.
(5) Schwall, G. P.; Safford, R.; Westcott, R. J.; Jeffcoat, R.; Tayal, A.; Shi, Y. C.; Gidley, M. J.; Jobling, S. A. Production of very-high-amylose potato starch by inhibition of SBE A and B. *Nat. Biotechnol.* **2000**, *18*, 551−554.

(6) Kang, H. J.; Hwang, I. K.; Kim, K. S.; Choi, H. C. Comparative structure and physicochemical properties of Ilpumbyeo, a high-quality Japonica rice, and its mutant, Suweon 464. *J. Agric. Food Chem.* **2003**, *51*, 6598−6603.
(7) Bird, A. R.; Jackson, M.; King, R. A.; Davies, D. A.; Usher, S.; Topping, D. L. A novel high-amylose barley cultivar (*Hordeum vulgare* var. Himalaya 292) lowers plasma cholesterol and alters indices of large-bowel fermentation in pigs. *Br. J. Nutr.* **2004**, *92*, 607−615.
(8) Regina, A.; Bird, A.; Topping, D.; Bowden, S.; Freeman, J.; Barsby, T.; Kosar-Hashemi, B.; Li, Z.; Rahman, S.; Morell, M. High-amylose wheat generated by RNA interference improves indices of large-bowel health in rats. *Proc. Natl. Acad. Sci. U.S.A.* **2006**, *103*, 3546−3551.
(9) Yang, C. Z.; Shu, X. L.; Zhang, L. L.; Wang, X. Y.; Zhao, H. J.; Ma, C. X.; Wu, D. X. Starch properties of mutant rice high in resistant starch. *J. Agric. Food Chem.* **2006**, *54*, 523−528.
(10) Jiang, H.; Campbell, M.; Blanco, M.; Jane, J. Characterization of maize amylose-extender (ae) mutant starches. Part II: Structures and properties of starch residues remaining after enzyme hydrolysis at boiling-water temperature. *Carbohydr. Polym.* **2010**, *80*, 1−12.
(11) Kim, K. S.; Hwang, H. G.; Kang, H. J.; Hwang, I. K.; Lee, Y. T.; Choi, H. C. Ultrastructure of individual and compound starch granules in isolation preparation from a high-quality, low-amylose rice, Ilpumbyeo, and its mutant, G2, a high-dietary fiber, high-amylose rice. *J. Agric. Food Chem.* **2005**, *53*, 8745−8751.
(12) Buléon, A.; Colomna, P.; Planchot, V.; Ball, S. Starch granules: Structure and biosynthesis. *Int. J. Biol. Macromol.* **1998**, *23*, 85−112.
(13) Cheetham, N. W. H.; Tao, L. Variation in crystalline type with amylose content in maize starch granules: An X-ray powder diffraction study. *Carbohydr. Polym.* **1998**, *36*, 277−284.
(14) Song, Y.; Jane, J. Characterization of barley starches of waxy, normal, and high amylose varieties. *Carbohydr. Polym.* **2000**, *41*, 365−377.
(15) Kim, K. S.; Kang, H. J.; Hwang, I. K.; Hwang, H. G.; Kim, T. Y.; Choi, H. C. Comparative ultrastructure of Ilpumbyeo, a high-quality Japonica rice, and its mutant, Suweon 464: Scanning and transmission electron microscopy studies. *J. Agric. Food Chem.* **2004**, *52*, 3876−3883.
(16) Jiang, H. X.; Horner, H. T.; Pepper, T. M.; Blanco, M.; Campbell, M.; Jane, J. Formation of elongated starch granules in high-amylose maize. *Carbohydr. Polym.* **2010**, *80*, 533−538.
(17) Zhu, L. J. Studies on starch structure and functional properties of high-amylose transgenic rice and different waxy rice varieties. Ph.D. Dissertation, Yangzhou University, Yangzhou, China, 2009.
(18) Wei, C. X.; Qin, F. L.; Zhu, L. J.; Zhou, W. D.; Chen, Y. F.; Wang, Y. P.; Gu, M. H.; Liu, Q. Q. Microstructure and ultrastructure of high-amylose rice resistant starch granules modified by antisense RNA inhibition of starch branching enzyme. *J. Agric. Food Chem.* **2010**, *58*, 1224−1232.
(19) Li, M.; Piao, J. h.; Liu, Q. Q.; Yang, X. G. Effects of the genetically modified rice enriched with resistant starch on large bowel health in rats. *Acta Nutr. Sin.* **2008**, *30*, 588−591.
(20) Wei, C. X.; Xu, B.; Qin, F. L.; Yu, H. G.; Chen, C.; Meng, X. L.; Zhu, L. J.; Wang, Y. P.; Gu, M. H.; Liu, Q. Q. C-Type starch from high-amylose rice resistant starch granules modified by antisense RNA inhibition of starch branching enzyme. *J. Agric. Food Chem.* **2010**, *58*, 7383−7388.
(21) Luft, J. H. Permanganate: A new fixative for electron microscopy. *J. Biophys. Biochem. Cytol.* **1956**, *2*, 799−802.
(22) Juliano, B. O. A simplified assay for milled-rice amylose. *Cereal Sci. Today* **1971**, *16*, 334−340.
(23) Nara, S.; Komiya, T. Studies on the relationship between water-saturated state and crystallinity by the diffraction method for moistened potato starch. *Starch/Staerke* **1983**, *35*, 407−410.
(24) Wei, C. X.; Zhang, J.; Zhou, W. D.; Chen, Y. F.; Liu, Q. Q. Degradation of amyloplast envelope and discussion on the concept of compound starch granule in rice endosperm. *Chin. J. Rice Sci.* **2008**, *22*, 377−384.
(25) Olsen, O. A.; Linnestad, C.; Nichols, S. E. Developmental biology of the cereal endosperm. *Trends Plant Sci.* **1999**, *4*, 253−257.
(26) Shannon, J. C.; Garwood, D. L. Genetics and physiology of starch development. In *Starch: Chemistry and Technology*; Whistler, R. L., Bemiller, J. N., Paschall, E. F., Eds.; Academic Press: New York, 1984; pp 25−86.
(27) Yoshida, M.; Fujii, M.; Nikuni, Z.; Maruo, B. The appositive growth of starch granules in beans as revealed by autoradiography. *Bull. Agric. Chem. Soc.* **1958**, *21*, 127.
(28) Dian, W.; Jiang, H.; Wu, P. Evolution and expression analysis of starch synthase III and IV in rice. *J. Exp. Bot.* **2005**, *56*, 623−632.
(29) Jane, J.; Xu, A.; Radosavljevic, M.; Seib, P. A. Location of amylose in normal starch granules. I. Susceptibility of amylose and amylopectin to cross-linking reagents. *Cereal Chem.* **1992**, *69*, 405−409.

Received for review June 30, 2010. Revised manuscript received August 28, 2010. Accepted September 10, 2010. This study was financially supported by grants from the National Natural Science Foundation of China (30828021, 30971754, and 31071342), the Ministry of Science and Technology (2009ZX08011-003B and 2008ZX08009-003), the Natural Science Foundation of Jiangsu Province (BK2009186), and the China Postdoctoral Science Foundation (20090451252).